Redox Biology 4 (2015) 363–374

Contents lists available at ScienceDirect

Redox Biology

journal homepage: www.elsevier.com/locate/redox

Research Paper

Neonatal iron supplementation potentiates oxidative stress, energetic dysfunction and neurodegeneration in the R6/2 mouse model of Huntington's disease

Kiersten L. Berggren [a], Jianfang Chen [a,b], Julia Fox [a], Jonathan Miller [a], Lindsay Dodds [a], Bryan Dugas [a], Liset Vargas [a], Amber Lothian [c], Erin McAllum [c], Irene Volitakis [c], Blaine Roberts [c], Ashley I. Bush [c], Jonathan H. Fox [a,b,*]

[a] Department of Veterinary Sciences, University of Wyoming, 1174 Snowy Range Road, Laramie, WY 82070, USA
[b] Neuroscience Graduate Program, University of Wyoming, 1174 Snowy Range Road, Laramie, WY 82070, USA
[c] Florey Institute of Neuroscience and Mental Health, University of Melbourne, Parkville, Victoria 3010, Australia

ARTICLE INFO

Article history:
Received 27 January 2015
Received in revised form
4 February 2015
Accepted 5 February 2015
Available online 11 February 2015

Keywords:
Huntington's
Iron
Neurodegeneration
Oxidative stress
Stereology
Gene environment interaction

ABSTRACT

Huntington's disease (HD) is a progressive neurodegenerative disorder caused by a CAG repeat expansion that encodes a polyglutamine tract in huntingtin (htt) protein. Dysregulation of brain iron homeostasis, oxidative stress and neurodegeneration are consistent features of the HD phenotype. Therefore, environmental factors that exacerbate oxidative stress and iron dysregulation may potentiate HD. Iron supplementation in the human population is common during infant and adult-life stages. In this study, iron supplementation in neonatal HD mice resulted in deterioration of spontaneous motor running activity, elevated levels of brain lactate and oxidized glutathione consistent with increased energetic dysfunction and oxidative stress, and increased striatal and motor cortical neuronal atrophy, collectively demonstrating potentiation of the disease phenotype. Oxidative stress, energetic, and anatomic markers of degeneration were not affected in wild-type littermate iron-supplemented mice. Further, there was no effect of elevated iron intake on disease outcomes in adult HD mice. We have demonstrated an interaction between the mutant huntingtin gene and iron supplementation in neonatal HD mice. Findings indicate that elevated neonatal iron intake potentiates mouse HD and promotes oxidative stress and energetic dysfunction in brain. Neonatal-infant dietary iron intake level may be an environmental modifier of human HD.

Introduction

Huntington's disease (HD) is a progressive autosomal dominant neurodegenerative disorder caused by a CAG repeat expansion in exon-1 of the huntingtin (htt) gene [1]. Disease onset is typically in early adult life with a range from childhood to advanced age. Degeneration occurs primarily in striatum and cerebral cortex [2]. Clinical signs of HD include involuntary movements dominated by chorea, cognitive decline, executive dysfunction and weight loss. CAG expansion size is the main determinant of HD age of onset [3] and is an important modifier of progression [4]. Non-huntingtin genetic variability and environmental factors explain the remaining variability in HD; however, specific genes and environmental factors are poorly defined [5].

Mutant htt protein mediates its neurodegeneration promoting effects though pathways that include transcriptional dysregulation, energetic dysfunction and oxidative stress [6–8]. Mutant htt expression in HD brain results in elevated brain regional iron and accumulation within neurons [9–11]. Iron is redox active and tight homeostatic regulation is needed to prevent generation of reactive oxygen species [12,13]. Dysregulation of iron homeostasis in HD may therefore contribute to disease progression by promotion of oxidative stress and interfere with diverse redox regulated pathways [14,15]. Iron homeostasis is mediated by the coordinated activity of import, export and transport proteins whose levels are regulated by whole body/brain iron status via iron-sensing proteins [16]. Expression of some of these proteins is altered in mouse

* Corresponding author at: Department of Veterinary Sciences, University of Wyoming, 1174 Snowy Range Road, Laramie, WY 82070, USA.
E-mail addresses: kberggre@uwyo.edu (K.L. Berggren), chenjianfang11@gmail.com (J. Chen), jfox8@uwyo.edu (J. Fox), jmill129@uwyo.edu (J. Miller), ldodds917@gmail.com (L. Dodds), dugas@uw.edu (B. Dugas), lvargas1@uwyo.edu (L. Vargas), irene.volitakis@florey.edu.au (I. Volitakis), blaine.roberts@florey.edu.au (B. Roberts), ashleyib@unimelb.edu.au (A.I. Bush), jfox7@uwyo.edu (J.H. Fox).

http://dx.doi.org/10.1016/j.redox.2015.02.002

HD brain [10]. Further, experimental drugs with iron-binding properties provide some protection in HD mice [10,17] supporting a role of iron in HD onset and/or progression. Despite these findings, the extent to which deregulated iron metabolism contributes to HD progression is unclear.

Iron, being an essential micronutrient, could influence HD through dietary intake level. This possibility is relevant to human HD because iron intake can vary widely in human infants through the use of natural or iron-fortified milk and in adults via diet and supplements. Neonatal mice supplemented with iron have decreased performance in neurobehavioral tests and increased iron content in the basal ganglia as adults [18,19]. Further, neonatal iron supplementation at a level equivalent to that found in iron-fortified milk replacers results in potentiating effects on brain aging and MPTP-induced Parkinsonism in mice [20]. Adult rats fed a two-fold increase in dietary iron had significantly increased iron levels in the striatum and altered brain glutathione consistent with oxidative stress [21]. Despite evidence that elevated iron intake can modify brain functions the relationship between iron nutrition, peripheral and central iron status, and HD progression is unknown.

The purpose of this study was to determine if elevated iron intake promotes HD as measured by markers of oxidative and energetic dysfunction, behavior and anatomic neurodegeneration. Elevated iron nutrition was studied during the neonatal and adult-life stages. The neonatal-life stage is a time of potential vulnerability to environmental effects on brain development that may impact the brain in adulthood [22]. In the adult-life stage there could be direct effects of dietary iron intake on neurodegeneration. We used R6/2 HD mice as they recapitulate the human brain iron phenotype and demonstrate rapid disease progression [10]. Increased iron intake during the neonatal period potentiated HD, as determined by behavioral, oxidative and energetic stress markers and quantitative neuropathology outcomes; effects of iron on neonatal wild-type mice were negligible. Further, there was no effect of adult iron supplementation on disease progression. The findings demonstrate a novel genotype by environment interaction in neonatal HD mice and suggest that iron intake level during the neonatal period may be an environmental modifier of human HD.

Materials and methods

Mouse maintenance

R6/2 HD mice were maintained by backcrossing HD males with B6/CBA F1 females. Tails were cut at approximately 3 weeks of age for genotyping. Mice were weaned at 3.5 weeks. Animals were maintained in a 12-h alternating dark-light cycle. Access to food and water was ad libitum. Each cage had a single mouse igloo® (Bio-Serv) and Sani Chip bedding (Harlan). CAG repeat sizes were monitored. Mice used in the neonatal iron supplementation study had a CAG repeat size in the range 180–185. Mice used in the adult iron supplementation study had a CAG repeat size in the range 150–160. The neonatal study was conducted first; due to expanding CAG repeat size in the colony, the adult study was conducted with a newly established colony. Based on previous studies in R6/2 mice, the target group sizes for behavioral studies were 10–16 animals, and for biochemistry and neuropathology studies 8–10 animals.

Experimental design and iron treatments

Female mice only were used in experiments as male mice were kept for breeding. In the neonatal iron supplementation study, mouse pups were administered 120 μg/g/day body weight carbonyl iron or saline via oral gavage from post-natal days 10–17. This dose has been used previously to model the feeding of a human infant with an iron-fortified milk replacer [20]. Pups were weighed daily prior to each gavage. Whole litters of mice were randomly assigned treatments. Upon weaning pups were grouped into cages of mice with the same genotype and treatment. In the adult iron supplementation study female mice were assigned to treatment groups at weaning. The standard food (LabDiet® 5K67) was changed to treatment casein-based diets at 5 weeks of age and mice were maintained on these until sacrificed. Iron specified diet contained 50 ppm (low/control), 150 ppm (medium) and 500 ppm (high) iron supplied as ferric citrate (Harlan). The 150 ppm concentration was chosen as this provides an equivalent level of iron to standard commonly used cereal-based rodent diets; 50 ppm is a low iron level but not sufficient to result in iron deficiency; and, 500 ppm was chosen to model a high-iron diet. The levels of iron supplementation over basal iron intake were chosen based on likely upper levels of iron supplementation in the human population at different life stages. Based on absence of premature mortality we found no evidence that iron dosing in either the neonatal or the adult study resulted in toxicity.

Behavioral analyses

Spontaneous cage wheel running activity was used as a measure of spontaneous activity as previously described [23]. Mice were placed individually in cages with wireless running wheels (Med Associates, Inc.) for 4 days. Data from days 2–4 was analyzed. Mice were then returned to their home cages. Wheel analyses were conducted at 5 and 10 weeks of age in the neonatal study, and at 4, 9, and 12 weeks of age in the adult study. These time points were chosen in order to establish baseline behavioral performance and to evaluate behavioral deterioration at various stages of disease progression.

Accelerating rotarod was used to evaluate for motor endurance. The rod accelerated from 5 to 25 rpm over 15 min. For each time point there was an initial training day in which mice were placed on the rota-rod for 5 min; mice that fell off were replaced on the rotating rod. Data were collected on the subsequent 3 days. Mice were placed on the rota-rod apparatus and were replaced on the apparatus if a fall occurred within the first 30 s of training. If a mouse fell a second time within the first 30 s the time was recorded and the trial ended. Any fall occurring after the initial 30 s of the trial was recorded as the latency to fall. Mice were tested on the rotarod at 5, 8, and 12 weeks of age in the neonatal study; in the adult study mice were tested at 4.5, 8, 10, and 12 weeks of age.

Quantitative neuropathology and huntingtin aggregate analysis

Stereological analyses of neuronal cell body volumes was completed using the Stereo Investigator software (MBF Bioscience, Williston, VT) as described previously [24]. In brief, mice were perfused for 3 min with heparinized 0.9% (w/v) saline then with 4% paraformaldehyde in 0.1 M phosphate buffer (pH 7.4) for 15 min. Brains were post-fixed for 24 h then cryopreserved in 10% glycerol, 2% DMSO and 0.1 M phosphate buffer for 5 days. Brains were sectioned frontally at 40 μm and stored in phosphate buffer. For Cavalieri estimation of striatal volume every 12th section was mounted on a glass slide and stained using the thionin method. Slides were letter-coded for blinding purposes. For nucleator estimation of striatal neuronal cell body volume a section at the level of the anterior commissure only was analyzed. To quantify mutant huntingtin aggregates we stained sections of striatum at the levels of the anterior commissure. Sections were stained while 'floating' using a 1:1000 dilution of anti-huntingtin antibody (MAB5374, Millipore) for 48 h; this was followed by a 24-h incubation in a

1:500 dilution AF488-labeled secondary antibody (Invitrogen). We used fluorescent Nissl Neurotrace® 640/660 (Invitrogen) to detect neuron cell bodies. Z-stacks in dorso-medial and mid-lateral striatum were captured using a Zeiss 710 confocal microscope and 60× oil objective then imported into stereo-investigator. Aggregates were counted using the optical fractionator method with a counting frame size of $25 \times 25\ \mu m^2$ and grid size of $67 \times 67\ \mu m^2$. All neurons and aggregates falling within the counting frame were counted separately. The proportion of neurons with aggregates for the different HD groups was analyzed.

Western blot analysis

Mice were anesthetized then transcardially perfused with 0.9% (w/v) saline containing 25 units/mL of heparin. Brains were removed, dissected and frozen at −80 °C. Weighed brain regions were homogenized in 12 volumes of a buffer comprising 20 mM Tris (pH 7.5), 150 mM NaCl, 1% triton-X100 and a protease inhibitor cocktail (Roche). Samples were then centrifuged for 12 min at 16,000*g* then supernatants aliquoted and stored at −80 °C. Twenty micrograms of protein was separated by reducing SDS-PAGE using 4–12% gradient gels then transferred to PVDF. Primary antibody concentrations were: transferrin receptor (Invitrogen; 1:500), amyloid precursor protein (Millipore; 1:1000) and actin (Sigma; 1:2000). HRP labeled secondary antibodies were used at 1:2000 dilution. Film was used for detection.

Oxidative and energetic markers

Glutathione (GSH) and oxidized glutathione (GSSG) were measured as described previously [25]. Lactate was measured as we have described previously [25,26].

Iron-analysis

Inductively-coupled-plasma mass spectroscopy (ICP-MS) was used to quantify iron levels in brain and liver. Mice were perfused with saline as described above. Dissected tissue was frozen then weighed prior to ICP-MS analysis as described previously [10,27]. Size-exclusion chromatography ICP-MS (SEC-ICP-MS) was used to quantify the amount of iron associated with the ferritin iron-storage protein fraction in brain. Frontal cortices were obtained as described for Western blot analysis then homogenized in 20 mM TRIS (pH 7.4), 100 mM NaCl and EDTA-free protease inhibitors (Roche) at a ratio of 1:4 (w/v) with polypropylene pestle. The protein concentration within the clarified supernatant was determined by measuring absorbance at 280 nm using a NanoDrop spectrophotometer (Thermo, Fisher Scientific). Metalloproteomic analysis was conducted as previously described [28,29]. In brief, samples were normalized to the same protein concentration then 120 μg was injected on to a Bio-SEC 3 size-exclusion column ($4.6 \times 150\ mm^2$, 3 μm 150 Å, Agilent). The samples were maintained at 4 °C prior to injection using a Peltier cooler autosampler (Agilent 1200 series). The column was developed using 200 mM NH_4NO_3 (trace metal basis, Sigma) (pH 7.8) with 10 μg/L of Cs and Sb as internal standard at a flow rate of 0.4 mL/min and 30 °C. The effluent from the column passed through a variable wavelength detector (280 nm) before being directly plumbed to an Agilent Technologies 7700× ICP-MS fitted with a Mira Mist nebulizer (Burgener research Inc., Ontario). The ICP-MS was operated using helium as a collision gas (3.4 mL/min) to remove polyatomic interferences. The ICP-MS was tuned daily using 1 μg/L Li, Co, Y, Ce and Tl standard. The individual integration time for each element was 0.1 s with a cycle time of 1.8 s. A standard curve for iron (2000–60,000 pg) was developed using ferritin (GE healthcare) dissolved in 0.1 M TRIS, pH 7.5. The concentration of iron in ferritin was determined by standard bulk analysis techniques.

Serum iron and transferrin saturation

Blood was collected from heart following anesthesia but prior to saline perfusions. Samples were centrifuged for 10 min at 5000*g* then serum stored at 4 °C. Analyses were completed within 2 weeks. We used an iron/transferrin saturation kit that utilizes the ferrozine method (Pointe Scientific, Inc.) and followed the manufacturer's instructions.

Statistical analyses

All data were analyzed using SAS software version 9.2 (Cary, NC). The GLM procedure was used for one-way ANOVA (brain iron, oxidized glutathione, lactate, huntingtin aggregates and cell body volumes). The MIXED procedure was used for repeated-measures analysis (rota-rod endurance and wheel running). Significant differences were determined by pre-planned pair-wise comparisons only if there were significant main effects or interactions in the overall analysis. Results are summarized as mean ± SEM (data had normal distribution and variances were homogenous) except for wheel running results which are provided as mean ± 95% confidence; these data were right-skewed and was analyzed following log transformation.

Results

Neonatal iron supplementation alters behavioral outcomes

Impaired motor performance is a consistent outcome in R6/2 HD mice [10,30–32]. We measured spontaneous motor activity by placing mice in cages with free access to a running wheel. There were no differences in wheel-running behavior between iron and saline-treated R6/2 and wild-type mice at 5 weeks of age consistent with absence of a toxic effect of the iron dose. However, at 10 weeks of age, corresponding to early advanced disease, neonatal iron-supplemented HD mice had significantly decreased activity compared to saline-treated HD in both light ($p=0.0010$) and dark ($p=0.0175$) phases (Fig. 1A and B). We also assessed motor endurance on the rota-rod. There was a sharp significant decline in rota-rod endurance in HD mice at 8 and 12 weeks; however, neonatal iron treatment did not affect Rota-rod performance in R6/2 HD mice (Fig. 1C), suggesting a possible floor effect. Survival analysis was not undertaken.

Neonatal iron treatment increases brain markers of oxidative stress

We analyzed three brain metabolite markers of redox and energetic state (GSH, GSSG, and lactate) in brain in 12-week-old mice to investigate if behavioral effects of iron supplementation in HD extend to involve established biochemical disease markers. Consistent with our previous report [25], GSSG was not elevated in the brains of control R6/2 HD compared to control wild-type mice at 12 weeks of age (Fig. 2A and B). However, neonatal iron supplementation resulted in significantly elevated GSSG in HD, but not wild-type mice, in both striatum ($p=0.0006$) and cortex ($p=0.0002$) (Fig. 2A and B). R6/2 HD mice had significantly elevated striatal and cortical GSH as we have reported previously (data not shown) [25]. However, there was no effect of neonatal iron supplementation on GSH in HD or wild-type mice; therefore the increase of GSSG is not secondary to increased GSH. GSH: total glutathione percent ratios in striatum and cortex were significantly decreased by neonatal iron supplementation in HD mice (HD control = 94.52 ± 0.48, HD iron = 92.52 ± 0.48, $p=0.0006$; and

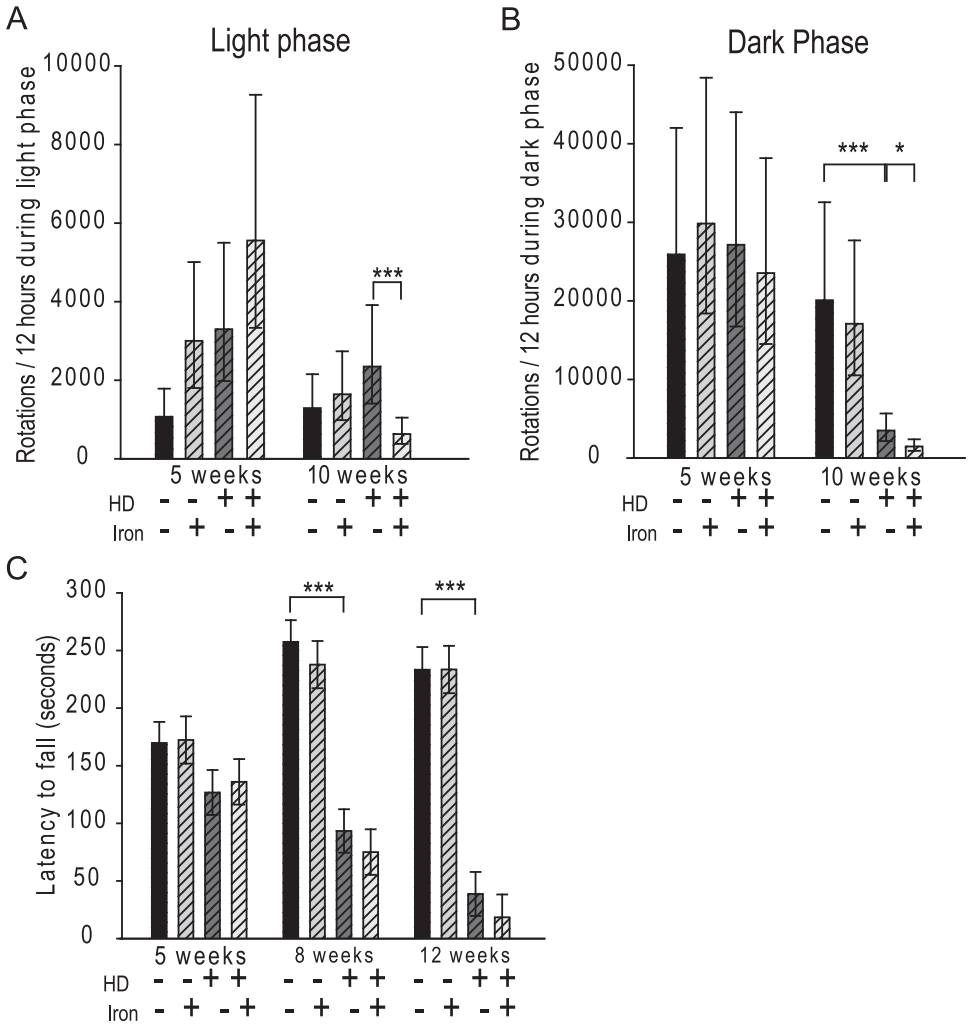

Fig. 1. Neonatal iron supplementation decreases spontaneous wheel activity in R6/2 HD mice but has no effect on rota-rod activity. (A and B) Spontaneous wheel activity in R6/2 and wild-type mice. Neonatal iron supplementation decreases spontaneous wheel activity in HD, but not wild-type mice, at 10 weeks of age in light (A) and dark (B) periods. Mutant huntingtin expression (HD) decreases spontaneous wheel activity at 10 weeks in the dark but not light. Bars represent mean ± 95% confidence intervals. (C) Rota-rod activity in R6/2 and wild-type mice. No effect of neonatal iron intake on rota-rod endurance. Graph bars: open=wild-type; hatched=HD; white=no supplementation; and gray=iron supplemented. $n=10$ for both studies. Asterisks indicate levels of significance: * <0.05, ** <0.01, *** <0.001.

HD control=96.52 ± 0.48, HD iron=95.19 ± 0.48, $p=0.0189$, respectively) but were not altered by iron treatment in wild-type mice (WT control=92.83 ± 0.48, WT iron=97.77, $p=0.9145$; and WT control=95.60 ± 0.48 WT iron=95.69 ± 0.48, $p=0.8788$, respectively). We also measured brain lactate in the current study to determine if changes in metabolic function are elicited by neonatal iron supplementation. While there was increased lactate in HD compared to wild-type mice, for reasons that are not clear, this was not significant in this study. Despite this, neonatal iron supplementation increased striatal ($p=0.0036$) and cortical ($p=0.0293$) lactate in HD, but not wild-type mice, when compared to respective controls (Fig. 2C and D).

Early-life iron treatment decreases neuronal volume and huntingtin aggregates in R6/2 mice

Neuronal cell body atrophy is a regular feature of mouse HD [30,33]; this outcome is a valuable anatomic marker of HD progression in pre-clinical therapeutic studies [24]. To determine if neonatal iron treatment exacerbated neuronal atrophy we quantified, using unbiased stereology, cell body volumes in striatum and layer V of primary motor cortex (Fig. 3). In striata (Fig. 3A and B) and motor cortex (C and D) cell body volumes were significantly decreased in HD controls compared to wild-type controls ($p=0.0323$ and 0.0279, respectively). Furthermore, iron supplementation resulted in further significant decreases in cell body volume in HD mice in striatum ($p=0.0246$) and primary motor cortex layer V ($p=0.0413$). There was no effect of iron supplementation in wild-type mice. We estimated striatal neuronal numbers using the optical fractionator stereological tool. While there was a significant decrease in neuronal numbers in HD mice [33] there was no effect of iron supplementation on estimates in wild-type or HD mice (not shown). Also, there was no effect of iron treatment on whole brain weights in HD or wild-type mice (not shown).

Mutant huntingtin protein aggregates are commonly found in mouse and human HD [34]. To investigate the effect of neonatal iron supplementation on huntingtin aggregates we used confocal microscopy and stereology to quantify neuronal cell body aggregates in striatum (Fig. 4A–C) and cortex (D–F). In striatum, compared to R6/2 HD controls (Fig. 4A), iron-supplemented R6/2 HD mice (B) had significantly fewer detectable neuronal huntingtin aggregates ($p=0.0279$). In motor cortex layer V, compared to the R6/2 control group (Fig. 4D), there was decreased neuronal

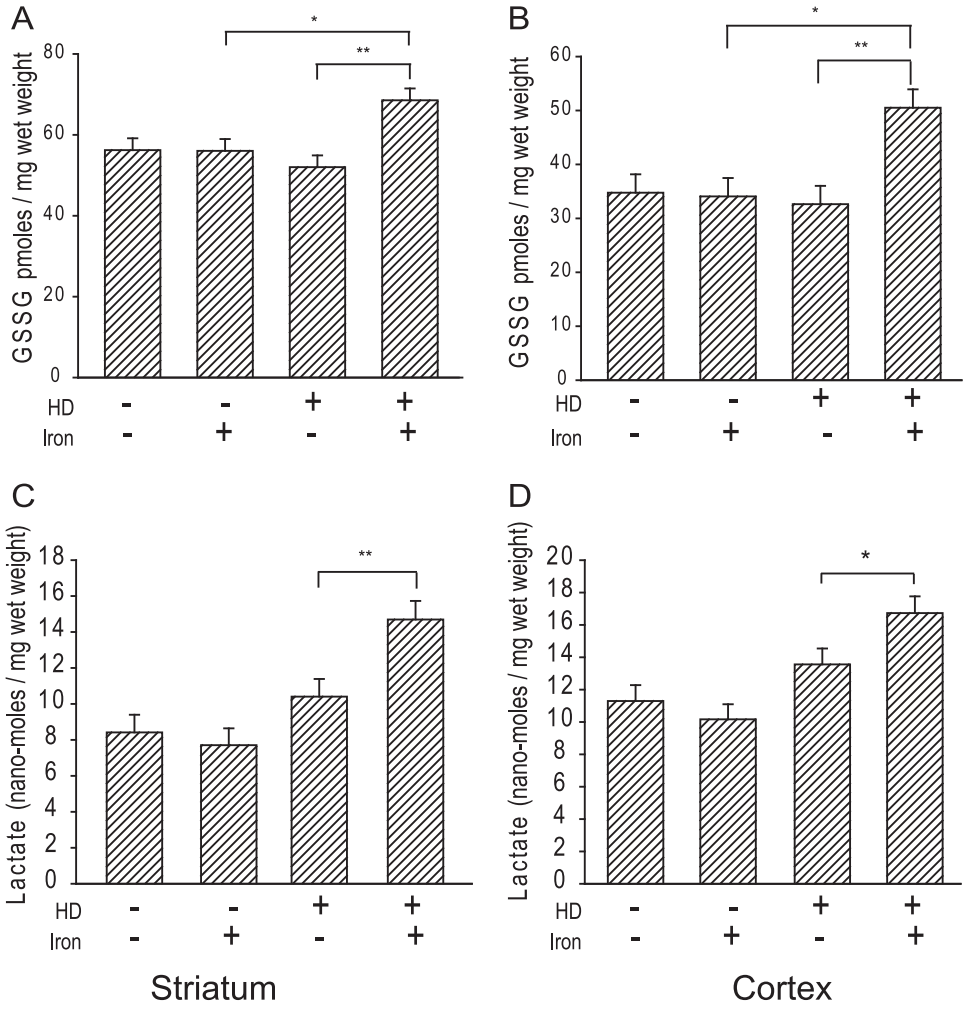

Fig. 2. Neonatal iron supplementation elevates markers of oxidative and energetic dysfunction in R6/2 HD but not wild-type mice. (A and B) Brain oxidized glutathione (GSSG) in neonatal iron supplemented mice. Supplementation increases striatal (A) and cortical (B) GSSG in HD, but not wild-type mice, at 12 weeks of age. GSSG levels are not affected by mutant huntingtin expression in striatum or cortex of 12-week-old R6/2 HD compared to wild-type mice. Asterisks indicate levels of significance: * <0.05, ** <0.01, *** <0.001, $n=10$. (C and D) Brain lactate in neonatal iron supplemented mice. Iron supplementation increases striatal (C) and cortical (D) lactate in HD, but not wild-type mice, at 12 weeks of age. Graph bars: open=wild-type; hatched=HD; white=no supplementation; and gray=iron supplemented. Asterisks indicate levels of significance: * <0.05, ** <0.01, *** <0.001, $n=10$.

aggregate burden in iron-supplemented R6/2 HD mice (E), but this difference did not reach statistical significance.

Brain iron status is unchanged by neonatal iron supplementation

We next addressed whether the potentiation of HD by iron supplementation (Figs. 1–4) associated with changes in brain iron status. First, we measured bulk brain regional iron levels. Consistent with previous findings, in striata (Fig. 5A) and frontal cortex (B), 12-week old R6/2 HD mice had significantly elevated iron compared to wild-type littermates ($p=0.0012$ and <0.0001). However, there was no effect of iron supplementation in HD mice. In wild-type mice only, iron supplementation did increase cortical iron ($p=0.0093$). Ferritin is an intra-cellular iron buffer and its iron content can increase with iron loading. We used size-exclusion chromatography combined with ICP-MS (SEC-ICP-MS) to quantify the amount of iron associated with the ferritin protein fraction in frontal cortex. We found that R6/2 HD mice had significantly more iron in the ferritin fraction as compared to wild-type mice (Fig. 5C) ($p=0.0003$); however, there was no effect of iron supplementation. To address the possibility that there may be transient elevated brain iron early in life we measured striatal (Fig. 5D) and cortical (E) iron in 5-week-old mice following neonatal dosing. There was no effect of iron supplementation on brain iron levels. We also measured brain copper and manganese. Copper and manganese concentrations were increased in HD mice compared to wild-type mice; however, there was no effect of iron supplementation on copper or manganese status (see Table 1). To further investigate whether neonatal iron treatment affected brain iron status in HD mice we quantified the levels of the iron-responsive proteins amyloid precursor protein (APP) and transferrin receptor (TfR). We have previously reported that levels of both APP and TfR are decreased in R6/2 HD brain [10]. APP promotes iron export from cells by stabilizing ferroportin [35,36]. We found decreased APP in striatum (Fig. 5F) ($p=0.0288$) and cortex (G) ($p=0.0149$) in HD mice compared to wild-type mice. The transferrin receptor was not decreased in striatum of R6/2 HD mice (Fig. 5H) but was deceased in cortex (I) ($p<0.0001$). There was no evidence of any effect of neonatal iron supplementation on APP or TfR in wild-type or R6/2 HD mice (Fig. 5F–I).

Given the absence of evidence to support a direct effect of neonatal iron supplementation on brain iron homeostasis we investigated how supplementation changes the peripheral environment. Specifically, we measured peripheral markers of iron and

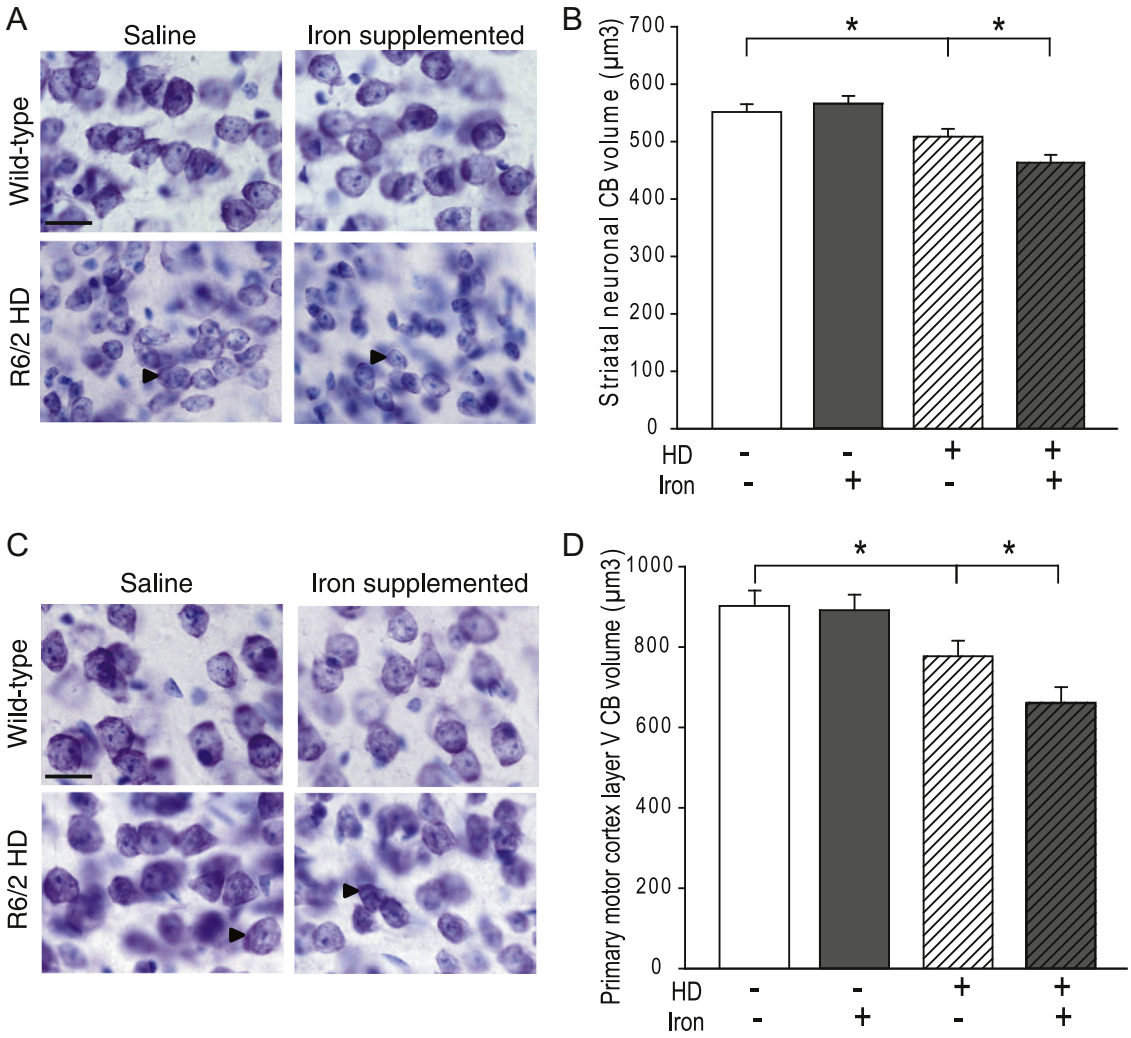

Fig. 3. Neonatal iron supplementation results in neuronal cell body atrophy in striatum and motor cortex in R6/2 HD but not wild-type mice. (A–D) Neuronal cell body size in neonatal iron supplemented mice. (A and B) R6/2 HD mice have significantly smaller striatal neuronal cell body size as compared to wild-type mice at 13 weeks of age. Neonatal iron supplementation decreases striatal neuronal cell body volume in R6/2 HD, but not wild-type mice, at 13 weeks of age. (C and D) R6/2 HD mice have significantly smaller neuronal cell body volume in primary motor cortex layer V as compared to wild-type mice at 13 weeks of age. Neonatal iron supplementation decreases neuronal volume in primary motor cortex layer V in HD, but not wild-type, mice. Bar=20 μm. (A and C) Representative images from 40 μm Thionin-stained sections. (B and D) Quantification of cell body size. Arrowheads demonstrate size differences among neurons. Graph bars: open=wild-type; hatched=HD; white=no supplementation; and gray=iron supplemented. Asterisks indicate levels of significance: * <0.05, ** <0.01, *** <0.001, CB=cell body, $n=10$.

redox status (Fig. 6). Serum iron concentrations and transferrin saturation are widely used clinical markers of iron status. Serum iron was unaltered by HD (Fig. 6A). However, iron supplementation decreased serum iron at 5 weeks ($p=0.0003$) in both HD and wild-type mice. At 13 weeks of age there was no effect of iron supplementation (Fig. 6A). Transferrin saturation was increased in HD controls as compared to wild-type controls at 5 weeks of age ($p=0.0386$). Further, at this age neonatal iron treatment decreased transferrin saturation in both wild-type and HD mice (Fig. 6B) ($p=0.0037$ and 0.0206, respectively). However, at 13-weeks transferrin saturation was significantly increased in iron supplemented compared to control HD mice ($p=0.0263$). To understand this effect further we determined liver iron as liver can act as an iron store [16]. In 5-week old animals, iron supplementation increased liver iron levels in both R6/2 HD ($p<0.0001$) and wild-type littermates ($p<0.0001$). However, at 13 weeks of age, neonatal iron treatment significantly increased liver iron levels in R6/2 ($p<0.0001$), but not wild-type mice (Fig. 6C). Finally, we measured plasma total glutathione levels as a marker of redox state; differences between groups were not evident (Fig. 6D).

Adult iron treatment does not potentiate HD outcomes in R6/2 mice

We next investigated whether increased iron intake during adult life can potentiate HD in R6/2 mice. We compared the effects of two or three dietary iron levels in our experiments (Fig. 7). There was no effect of iron intake level on rota-rod endurance (Fig. 7A) or spontaneous wheel running activity (Fig. 7B) in HD mice. However, there was an age-dependent decline in rota-rod endurance in wild-type mice fed medium and high iron diets (Fig. 7A). Dietary iron level did not alter striatal or cortical oxidized glutathione levels in HD or wild-type 12-week-old mice (data not shown). R6/2 HD mice had elevated striatal and cortical lactate ($p=0.0002$ and <0.0001, respectively); however, there was no effect of iron intake on brain lactate (data not shown). R6/2 HD mice had decreased striatal neuronal volume ($p=0.0254$) but there was no effect of dietary iron level on this outcome (Fig. 7C). There was also no effect of iron treatment on neuronal mutant huntingtin aggregates in HD mice (Fig. 7D). Bulk iron levels were increased in striatum (Fig. 7E) and cortex (F) in HD mice ($p<0.0001$ and 0.0020, respectively); however, there was no

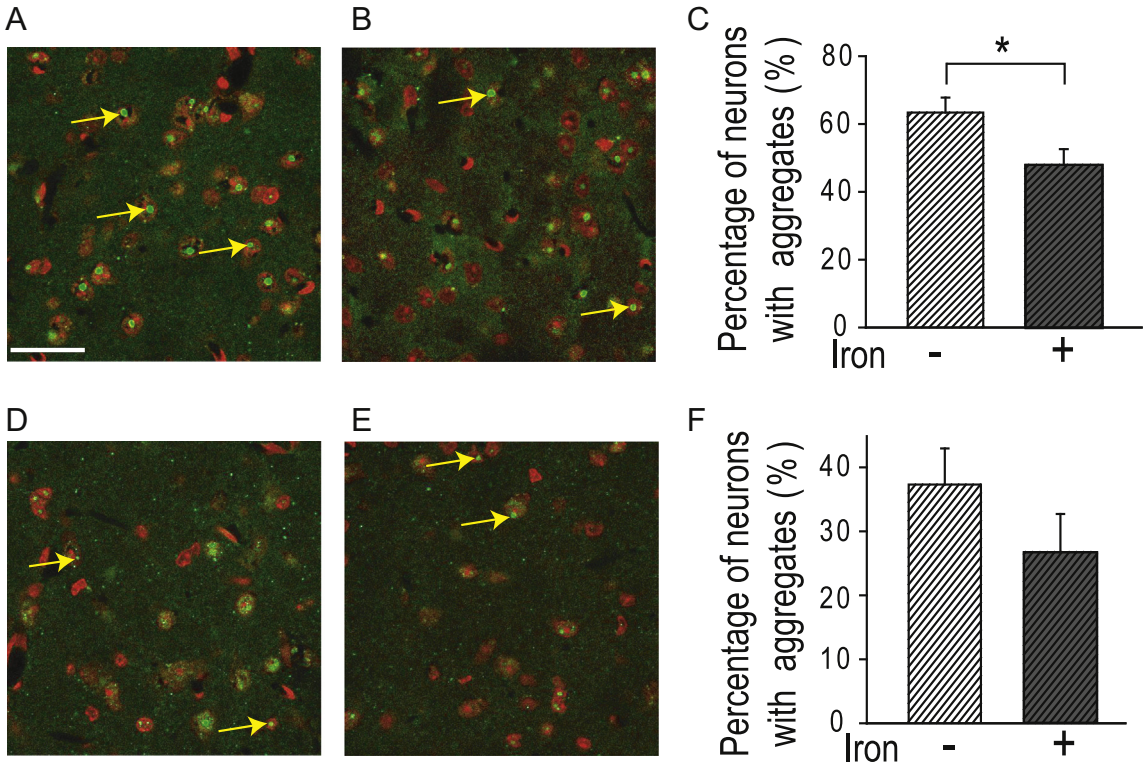

Fig. 4. Neonatal iron supplementation decreases mutant huntingtin aggregate load in R6/2 HD striata. Mutant aggregate load was quantified by confocal microscopy in striatum (A–C) and primary motor cortex layer 6 (D–F) of R6/2 HD mice at 13 weeks of age. The percentage of HD striatal neuronal cell bodies (red) containing microscopically visible aggregates (green) is significantly decreased in neonatal iron supplemented (B) as compared to control (A) HD mice. There is decreased mutant huntingtin aggregate load in motor cortex of neonatal iron supplemented (E) compared to control (D) HD mice, but this difference was not statistically significant. Bar=20 μm. Graph bars: hatched=HD; white=no supplementation; and gray=iron supplemented. Asterisks: * <0.05, $n=10$.

effect of iron treatment on brain iron. Finally, we determined transferrin saturation as a peripheral marker of iron status. In HD mice, transferrin saturation was decreased with elevated dietary iron intake ($p=0.0187$) (Fig. 7G).

Discussion

R6/2 HD mice express the exon-1 fragment of polyglutamine-expanded human huntingtin protein (htt) [37]. They develop advanced disease by 12 weeks of age and demonstrate many features found in human HD at the motor function, brain pathology and molecular levels. Therefore, R6/2 HD mice represent a model of rapidly developing HD that is valuable for studying disease modifying interventions. Here we show that neonatal iron supplementation potentiates R6/2 mouse HD as measured by behavioral, neuropathological and biochemical outcomes (Figs. 1–5). Effects of iron supplementation were not present in early-adult life (5 weeks) consistent with an absence of iron toxicity, but were manifest with early-advanced HD at 12 weeks of age (Fig. 1). Importantly, the effects of neonatal iron supplementation did not occur in wild-type litter-mate mice consistent with an interaction between the HD gene and iron intake. Iron supplementation had no effect in adult R6/2 HD mice (Fig. 7). The findings indicate that in this mouse model of HD the neonatal-life stage is a period of specific vulnerability to the effects of elevated iron intake.

Perinatal iron deficiency is a world-wide nutritional problem that can lead to delayed neurocognitive development [38]. During the neonatal-infant period, iron absorption is inefficient, brain growth is rapid and brain iron uptake is high; while mechanisms to maintain brain iron homeostasis are not fully developed (reviewed in [39]). Human milk replacer formulas typically contain levels of iron greater than that found in human milk, up to forty times more iron is present in some replacers [20]. Despite elevated iron intake from milk replacers, few studies have addressed the effect of elevated neonatal iron intake on brain aging and interactions with neurodegenerative diseases. In our neonatal mouse iron supplementation study, we used a level of iron estimated to provide forty times more iron than the mouse pup would have received naturally from mouse milk as previously reported [20]. Body surface area is an alternative, and perhaps preferable, approach to translate dose across species [40]. Using this method the dose we used in mice translates to less than a forty-fold increase in iron intake in a human infant. Based on brain developmental staging, dosing on days 10–17 is equivalent to an infant receiving iron supplementation from birth through 20 weeks [41]. Therefore, the dose and age of supplementation of iron we used in the neonatal study is relevant to human nutrition. Using this regimen, we found significant deleterious effects of neonatal iron supplementation in R6/2 mice that spanned behavioral (Fig. 1), biochemical markers of oxidative stress and energetic dysfunction (Fig. 2), and quantitative pathology (Fig. 3) domains. We additionally found that iron supplemented HD mice had fewer striatal aggregates (Fig. 4). While we did not measure soluble mutant htt levels, fewer aggregates are compatible with potentiated HD because neurons with fewer aggregates may have increased soluble mutant htt which is more toxic than aggregated mutant htt [42]. Taken together, the presence of effects of neonatal iron supplementation on multiple outcomes in HD mice suggests that similar effects of neonatal iron supplementation could occur in human HD.

Exacerbations of oxidative stress are common features of neurodegenerative diseases (reviewed in [43]). Glutathione (GSH) is an electron donor required for several enzyme systems

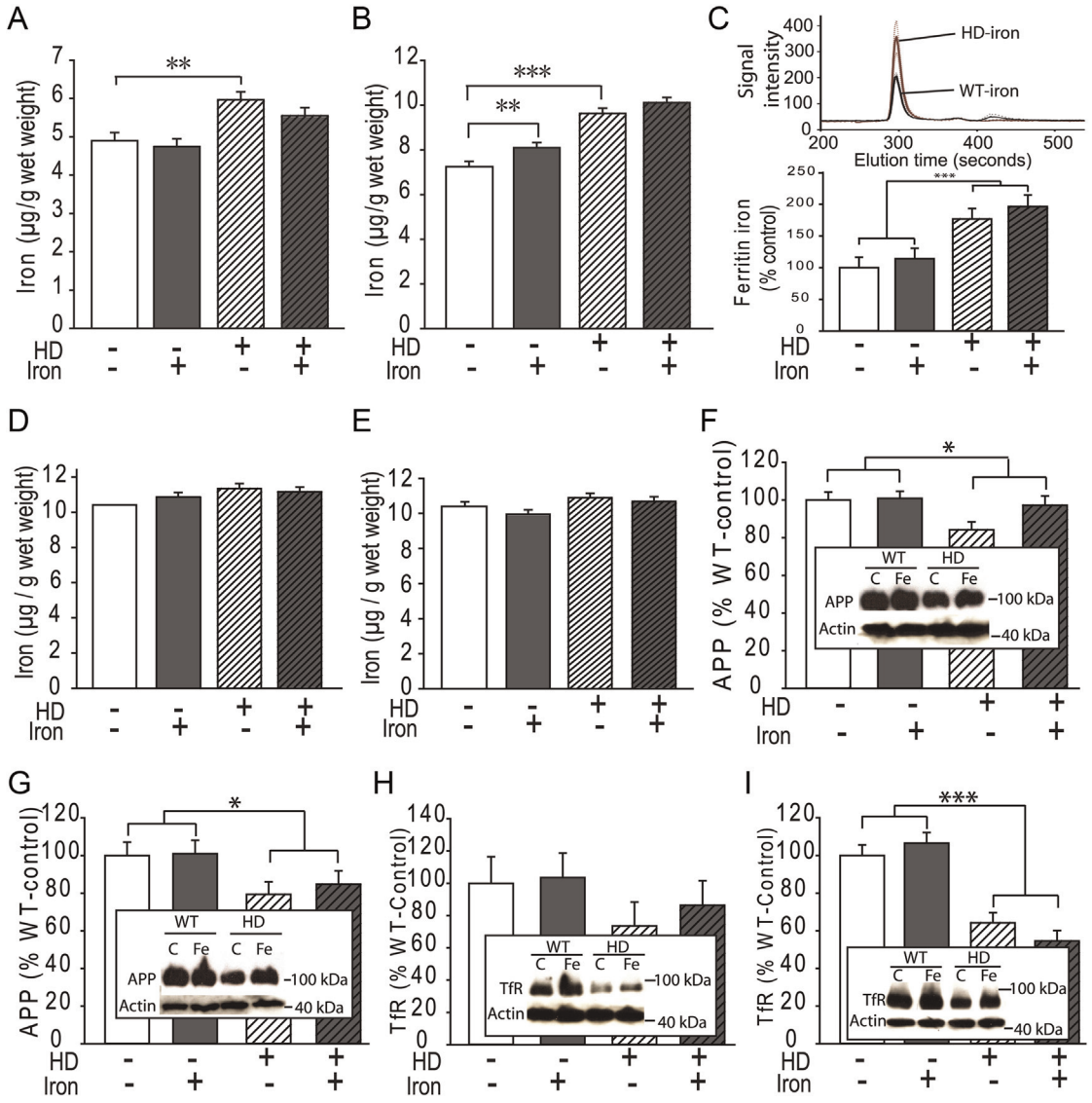

Fig. 5. Neonatal iron supplementation does not alter markers of brain iron status in HD mice. (A and B) Brain iron levels at 12 weeks of age. Iron levels are significantly elevated in striatum (A) and cortex (B) of 12-week-old R6/2 HD as compared to wild-type control mice. $n=10$–11. (B) Iron supplementation significantly increases cortical iron in wild-type control mice but not in R6/2 HD mice. (C) Iron levels associated with ferritin protein fraction in cortex at 12 weeks of age. Protein extracts from 12-week-old cortex were resolved by size-exclusion chromatography (SEC) followed by in-line ICP-MS for iron content. Solid line=mean; dotted line=standard error. There is a significantly increased iron content of the ferritin protein fraction in R6/2 HD mice. There is no effect of iron supplementation on ferritin-associated iron. $n=5$. (D and E) Brain iron levels at 5 weeks of age. There is no effect of genotype or iron supplementation on striatal (D) or cortical (E) iron level. $n=10$–11. (F–I) Levels of iron-responsive proteins in HD mouse brain. (F and G) Amyloid precursor protein (APP) levels are significantly decreased in striata (F) and cortices (G) of HD mice. There is no effect of neonatal iron supplementation. (H and I) Transferrin receptor levels are decreased in cortex of HD mice compared to wild-type mice. There is no effect of neonatal iron supplementation in striatum (H) or cortex (I). Graph bars: open=wild-type; hatched=HD; white = no supplementation; and gray=iron supplemented. $n=7$–8, asterisks indicate the level of significance: * <0.05, ** <0.01, *** <0.001.

including glutathione peroxidases and glutaredoxins. In this process, GSH is oxidized to GSSG (oxidized glutathione), an indicator of oxidative stress. GSSG is increased in a cell line model of HD [44] and also the brains of N171-82Q HD mice [23]. We found that iron supplemented HD mice had significant increases in cortical and striatal GSSG. While HD mice had significantly increased cortical and striatal GSH compared to wild-type mice, this effect was not exacerbated by iron supplementation. Brain lactate is elevated in human HD and is one valuable marker for energetic dysfunction [45]. We have previously found elevated brain lactate in R6/2 HD mice [26]; the current findings show that iron supplementation increases brain lactate levels in HD but not wild-type mice. Taken together, these findings indicate a state of metabolic dysregulation in R6/2 HD mice.

Iron homeostasis requires the regulation of intestinal iron absorption, storage as ferritin, transport in blood and uptake by brain and other organs [16]. We have previously shown altered expression levels of the iron homeostatic proteins, transferrin receptor and amyloid precursor protein, in R6/2 HD brain [10,26]. Amyloid precursor protein promotes iron export from cells by stabilizing surface ferroportin [35,36]; decreased levels in R6/2 HD mice may explain elevated brain iron [10]. While brain and body iron homeostasis is tightly regulated, it is still modifiable by dietary iron intake. For example, early-life iron overload in mice has been shown to have significant effects on neurobehavioral performance [18,19]. Furthermore, neonatal iron supplementation in wild-type mice has been shown to alter brain iron levels in adult animals [18,20,46]. Consistent with these findings, we found increased cortical iron in 12-week-old wild-type mice that were supplemented as neonates (Fig. 5B). We were surprised however

that there was no increase in striatal or cortical iron in neonatally-supplemented HD mice (Fig. 5A and B). Furthermore, we found no evidence of changes in cortical iron status in HD mice using SEC-ICP-MS to quantify iron levels in the ferritin protein fraction (Fig. 5C). We additionally undertook Western blot analysis of the iron-responsive amyloid precursor protein and the transferrin receptor as an alternative approach to detect changes in brain iron homeostasis but did not detect effects of iron supplementation (Fig. 5F–I). Brain iron homeostasis is complex and we cannot rule out the possibility of undetected changes in brain iron including altered distribution within cell compartments. We investigated peripheral iron and redox status as an alternative path to modification of HD (Fig. 6). Findings reveal that R6/2 HD mice, compared to wild-types, have unaltered serum iron but that there is an early and transient decrease in serum iron at 5 weeks in iron supplemented mice, that is absent at 13 weeks (Fig. 6A). This appears to be explained by the increase in iron sequestration by liver at this age (Fig. 6C). Transferrin saturation was decreased at 5 weeks by iron supplementation; however, at 13-weeks iron-supplemented HD mice had elevated transferrin saturation

Table 1
Brain metal concentrations.

	Striatum				Cortex			
	WT-saline	**WT-iron**	**HD-saline**	**HD-iron**	**WT-saline**	**WT-iron**	**HD-saline**	**HD-iron**
Copper	2.11 (0.12)	1.94 (0.12)	2.43 (0.12)	2.43 (0.12)*	3.49 (0.12)	3.53 (0.12)	3.96 (0.12)**	3.96 (0.12)‡
Manganese	0.14 (0.01)	0.13 (0.01)	0.16 (0.01)$^{\#\#}$	0.15 (0.01)	0.33 (0.01)	0.32 (0.01)	0.39 (0.01)***	0.41 (0.01)$^{\#\#\#}$

Values represent concentrations in μg/g wet weight (standard error); WT=wild-type, HD=R6/2.

* $p<0.01$ vs. WT-iron.
** $p<0.01$ vs. WT-saline.
*** $p<0.001$ vs. WT-saline.
# $p<0.05$ vs. WT-iron.
$p<0.05$ vs. WT-iron.
$p<0.0001$ vs. WT-iron.

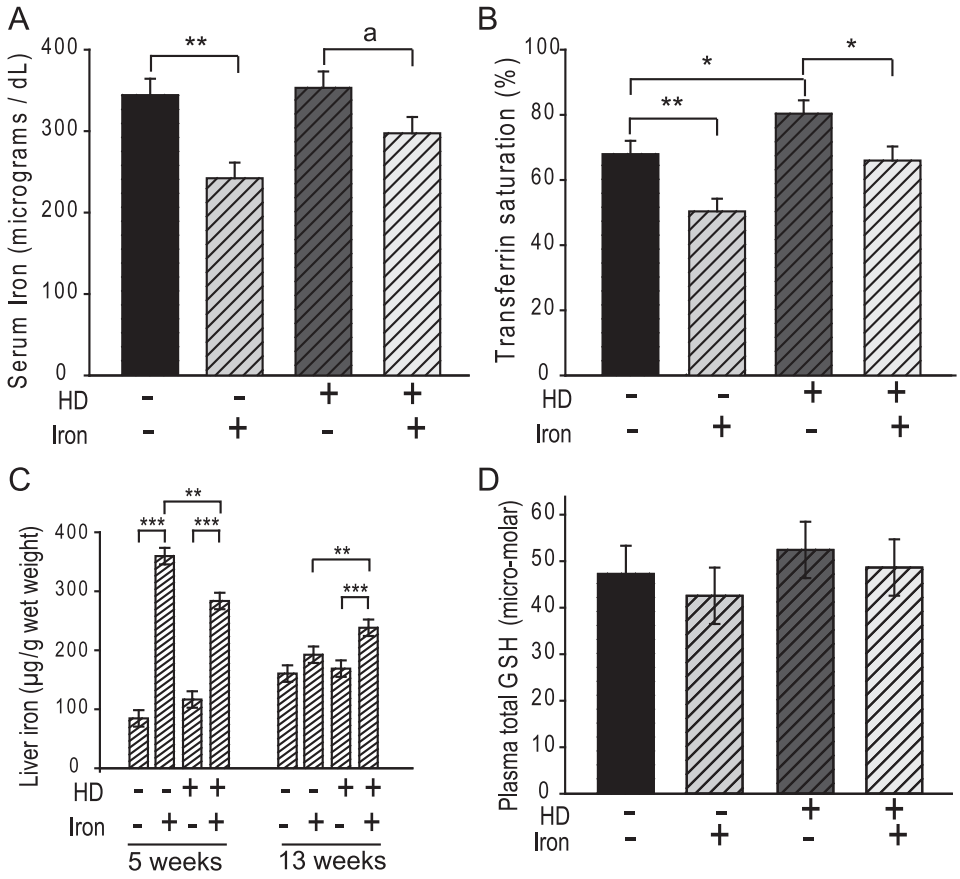

Fig. 6. Neonatal iron supplementation alters peripheral markers of iron status. (A and B) Serum iron status markers in iron-supplemented and control wild-type and HD mice at 5 and 13 weeks of age. $n=9$–10. (A) Serum iron levels are decreased by iron supplementation in wild-type and HD mice at 5 weeks (main effect $p=0.0003$; $a=0.0571$). There is no difference in serum iron in 12-week-old mice. (B) Serum transferrin saturation is increased in HD mice compared to wild-type litter-mate controls at 5 weeks. Iron supplementation decreases transferrin saturation in 5-week wild-type and HD mice. R6/2 HD mice supplemented with iron as neonates have increased transferrin saturation at 13 weeks. (C) Liver iron levels. Iron supplemented HD and wild-type litter-mate mice have elevated liver iron at 5 weeks of age; at 13 weeks liver iron is elevated in HD mice only. $n=10$–11. (D) There is no effect of genotype or iron supplementation on plasma total glutathione (GSH). Graph bars: open=wild-type; hatched=HD; white=no supplementation; and gray=iron supplemented. $n=10$, asterisks indicate the level of significance: * <0.05, ** <0.01, *** <0.001.

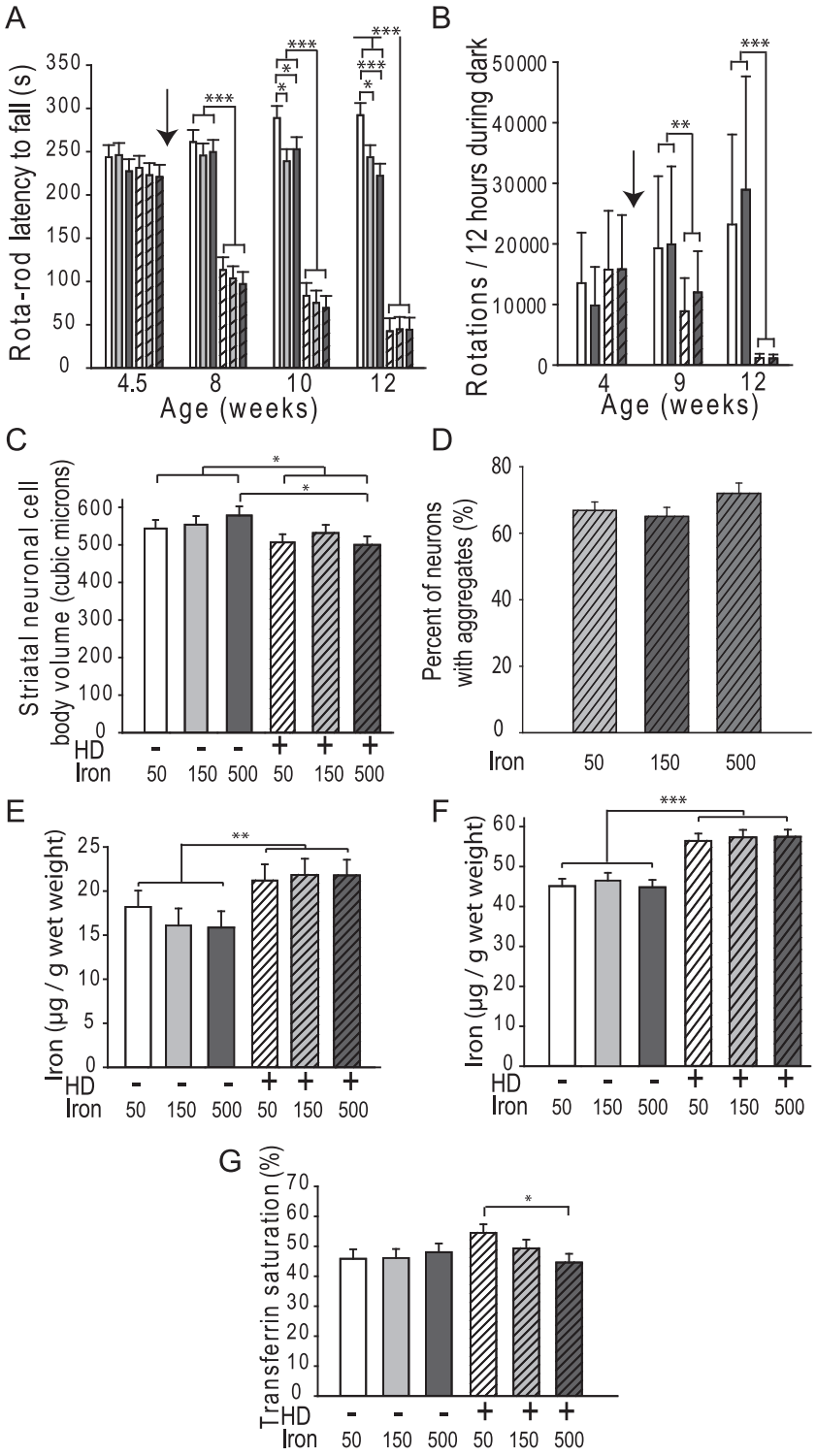

Fig. 7. Increased iron intake in adult R6/2 mice does not potentiate HD. (A–C) Motor performance testing in wild-type and R6/2 HD mice fed different levels of iron from 5 weeks of age. (A) HD mice perform significantly worse than wild-type litter-mate mice on a rota-rod motor endurance test. At each age graph bars, from left to right, represent iron levels in parts-per-million (ppm): wild-type (WT) 50 (white-hatched), WT 150 (gray-hatched), WT 500 (black), HD 50 (white-hatched), HD 150 (gray-hatched) and HD 500 (black). There is no effect of iron intake level in HD mice. Wild-type mice fed 150 and 500 ppm iron demonstrate age-dependent decline in rota-rod activity. $n=13$–15. (B) HD mice perform worse on a spontaneous wheel running test in the dark periods. There is no effect of iron intake level. At each age graph bars, from left to right, represent: WT 50 (white-hatched), WT 500 (black), HD 50 (white-hatched) and HD 500 (gray). $n=9$–10. (C) Striatal neuronal cell body volume is decreased in R6/2HD mice at 12 weeks of age, compared to wild-type litter mates. There is no effect of iron intake level. $n=8$–10. (D) There is no effect of iron intake level on mutant huntingtin aggregates in HD mice, $n=7$–10. (E and F) Iron concentrations in striatum (E) and frontal cortex (F) at are increased at 12 weeks of age; there is no effect of iron treatment. $n=10$–11. (G) Low iron intake results in increased transferrin saturation at 12 weeks of age in HD but not wild-type mice. $n=10$–12. Graph bars: open=wild-type and hatched=HD; dietary iron levels, white=50 ppm, light gray=150 ppm and dark gray=500 ppm. Asterisks indicate the level of significance: * <0.05, ** <0.01, *** <0.001.

(Fig. 6B). This later finding is consistent with decreased transferrin, but increased iron-loading of remaining transferrin suggesting dysregulation of peripheral iron regulation in HD. Overall, both wild-type and HD mice show similar short and longer term peripheral responses to iron supplementation. However, differences in these responses in HD mice show that mutant htt affects the systemic response to iron intake level; this different response may be involved in the mechanism of how neonatal iron supplementation potentiates HD and indicates a complex interplay between iron intake, huntingtin and systemic iron metabolism.

Multivitamin–multimineral (MVMM) supplements are used by about a third of the US population [47]. The recommended daily allowance of iron for all adult men and women over 50 is 8 mg [48]. Many generic MVMM tablets contain 18 mg iron, a level only recommended for women 19–50 years of age. There is therefore potential for over-supplementation in part of the population. Based on this, we investigated the effect of elevated iron intake in adult R6/2 HD mice. Even though there was a ten-fold difference between low and high dietary iron intake levels (see Materials and Methods section) we found no effect of iron intake level in R6/2 HD mice (Fig. 7). Wild-type mice fed the medium and high iron diets demonstrated some decline in rota-rod endurance (Fig. 7A); however, there was no other evidence for an effect of iron intake in wild-type mice. Unlike the neonatal iron supplementation study (Fig. 6B), adult iron supplementation did not elevate cortical iron levels in wild-type mice (Fig. 7E). However, there was a differential response of blood transferrin saturation between wild-type and HD mice (Fig. 7G) which is consistent with altered systemic responses to iron-loading in the neonatal study. Together these data suggest that dysregulation of peripheral iron homeostasis also occurs in adult HD mice.

Conclusions

Iron supplementation in neonatal HD mice potentiates the course of HD in R6/2 mice. Increased levels of brain oxidized glutathione and lactate were found in iron supplemented mice consistent with a role of oxidative stress and energetic dysfunction in disease potentiation. HD potentiation occurred in the absence of detectable changes in brain iron status demonstrating that iron's role in HD cannot be simply defined at the level of increased brain regional concentrations. The findings support a role of iron nutrition during early brain development as a modifier of HD. This period of developmental vulnerability to elevated iron intake could also be present in HD gene-positive infants. Prospective clinical investigation of this phenomenon in humans is challenging due to the usual adult age of HD clinical onset; however, retrospective or biomarker studies could allow further investigation of the relationship between neonatal iron intake and HD onset or progression.

Acknowledgments

Funding was provided by RO1 NS079450 from NINDS.

References

[1] THDCRG, A novel gene containing a trinucleotide repeat that is expanded and unstable on Huntington's disease chromosomes. The Huntington's Disease Collaborative Research Group, Cell 72 (6) (1993) 971–983. http://dx.doi.org/10.1016/0092-8674(93)90585-E 8458085.

[2] J.P. Vonsattel, R.H. Myers, T.J. Stevens, R.J. Ferrante, E.D. Bird, E.P. Richardson Jr., Neuropathological classification of Huntington's disease, Journal of Neuropathology and Experimental Neurology 44 (6) (1985) 559–577. http://dx.doi.org/10.1097/00005072-198511000-00003 2932539.

[3] R.G. Snell, J.C. MacMillan, J.P. Cheadle, I. Fenton, L.P. Lazarou, P. Davies, M. E. MacDonald, J.F. Gusella, P.S. Harper, D.J. Shaw, Relationship between trinucleotide repeat expansion and phenotypic variation in Huntington's disease, Nature Genetics 4 (4) (1993) 393–397. http://dx.doi.org/10.1038/ng0893-393 8401588.

[4] A. Rosenblatt, B.V. Kumar, A. Mo, C.S. Welsh, R.L. Margolis, C.A. Ross, Age, CAG repeat length, and clinical progression in Huntington's disease, Movement Disorders: Official Journal of the Movement Disorder Society 27 (2) (2012) 272–276. http://dx.doi.org/10.1002/mds.24024 22173986.

[5] L. Arning, J.T. Epplen, Genetic modifiers of Huntington's disease: beyond CAG, Future Neurology 7 (1) (2012) 93–109. http://dx.doi.org/10.2217/fnl.11.65.

[6] A.W. Dunah, H. Jeong, A. Griffin, Y.M. Kim, D.G. Standaert, S.M. Hersch, M. M. Mouradian, A.B. Young, N. Tanese, D. Krainc, Sp1 and TAFII130 transcriptional activity disrupted in early Huntington's disease, Science 296 (5576) (2002) 2238–2243. http://dx.doi.org/10.1126/science.1072613 11988536.

[7] L. Cui, H. Jeong, F. Borovecki, C.N. Parkhurst, N. Tanese, D. Krainc, Transcriptional repression of PGC-1alpha by mutant huntingtin leads to mitochondrial dysfunction and neurodegeneration, Cell 127 (1) (2006) 59–69. http://dx.doi.org/10.1016/j.cell.2006.09.015 17018277.

[8] A. Valencia, E. Sapp, J.S. Kimm, H. McClory, P.B. Reeves, J. Alexander, K. A. Ansong, N. Masso, M.P. Frosch, K.B. Kegel, X. Li, M. DiFiglia, Elevated NADPH oxidase activity contributes to oxidative stress and cell death in Huntington's disease, Human Molecular Genetics 22 (6) (2013) 1112–1131. http://dx.doi.org/10.1093/hmg/dds516 23223017.

[9] H.D. Rosas, Y.I. Chen, G. Doros, D.H. Salat, N.K. Chen, K.K. Kwong, A. Bush, J. Fox, S.M. Hersch, Alterations in brain transition metals in Huntington disease: an evolving and intricate story, Archives of Neurology 69 (2012) 887–893. http://dx.doi.org/10.1001/archneurol.2011.2945 22393169.

[10] J. Chen, E. Marks, B. Lai, Z. Zhang, J.A. Duce, L.Q. Lam, I. Volitakis, A.I. Bush, S. Hersch, J.H. Fox, Iron accumulates in Huntington's disease neurons: protection by deferoxamine, PLOS One 8 (10) (2013) e77023. http://dx.doi.org/10.1371/journal.pone.0077023 24146952.

[11] D.T. Dexter, A. Carayon, F. Javoy-Agid, Y. Agid, F.R. Wells, S.E. Daniel, A.J. Lees, P. Jenner, C.D. Marsden, Alterations in the levels of iron, ferritin and other trace metals in Parkinson's disease and other neurodegenerative diseases affecting the basal ganglia, Brain 114 (4) (1991) 1953–1975. http://dx.doi.org/10.1093/brain/114.4.1953 1832073.

[12] H.J.H. Fenton, Oxidation of tartaric acid in presence of iron, Journal of the Chemical Society, Transactions 65 (1894) 899–911. http://dx.doi.org/10.1039/ct8946500899.

[13] R.J. Ward, F.A. Zucca, J.H. Duyn, R.R. Crichton, L. Zecca, The role of iron in brain ageing and neurodegenerative disorders, Lancet Neurology 13 (10) (2014) 1045–1060. http://dx.doi.org/10.1016/S1474-4422(14)70117-6 25231526.

[14] C. Peers, J.P. Boyle, Oxidative modulation of K(+) channels in the central nervous system in neurodegenerative diseases and aging, Antioxidants & Redox Signaling (2014), http://dx.doi.org/10.1089/ars.2014.6007 25333910.

[15] B. Lizama-Manibusan, B. McLaughlin, Redox modification of proteins as essential mediators of CNS autophagy and mitophagy, FEBS Letters 587 (15) (2013) 2291–2298. http://dx.doi.org/10.1016/j.febslet.2013.06.007 23773928.

[16] T. Ganz, Systemic iron homeostasis, Physiological Reviews 93 (4) (2013) 1721–1741. http://dx.doi.org/10.1152/physrev.00008.2013 24137020.

[17] R.A. Cherny, S. Ayton, D.I. Finkelstein, A.I. Bush, G. McColl, S.M. Massa, PBT2 reduces toxicity in a *C. elegans* model of polyQ aggregation and extends lifespan, reduces striatal atrophy and improves motor performance in the R6/2 mouse model of Huntington's disease, Journal of Huntington's Disease 1 (2) (2012) 211–219. http://dx.doi.org/10.3233/JHD-120029 25063332.

[18] A. Fredriksson, N. Schröder, P. Eriksson, I. Izquierdo, T. Archer, Neonatal iron exposure induces neurobehavioral dysfunctions in adult mice, Toxicology and Applied Pharmacology 159 (1) (1999) 25–30. http://dx.doi.org/10.1006/taap.1999.8711 10448122.

[19] M.N. De Lima, D.C. Laranja, F. Caldana, M.M. Grazziotin, V.A. Garcia, F. Dal-Pizzol, E. Bromberg, N. Schröder, Selegiline protects against recognition memory impairment induced by neonatal iron treatment, Experimental Neurology 196 (1) (2005) 177–183. http://dx.doi.org/10.1016/j.expneurol.2005.07.017 16122736.

[20] D. Kaur, J. Peng, S.J. Chinta, S. Rajagopalan, D.A. Di Monte, R.A. Cherny, J. K. Andersen, Increased murine neonatal iron intake results in Parkinson-like neurodegeneration with age, Neurobiology of Aging 28 (6) (2007) 907–913. http://dx.doi.org/10.1016/j.neurobiolaging.2006.04.003 16765489.

[21] S. Yu, Y. Feng, Z. Shen, M. Li, Diet supplementation with iron augments brain oxidative stress status in a rat model of psychological stress, Nutrition 27 (2011) 1048–1052. http://dx.doi.org/10.1016/j.nut.2010.11.007 21454054.

[22] D. Rice, S. Barone Jr., Critical periods of vulnerability for the developing nervous system: evidence from humans and animal models, Environmental Health Perspectives 108 (Suppl. 3) (2000) 511–533 10852851.

[23] Z. Lu, E. Marks, J. Chen, J. Moline, L. Barrows, M. Raisbeck, I. Volitakis, R. A. Cherny, V. Chopra, A.I. Bush, S. Hersch, J.H. Fox, Altered selenium status in Huntington's disease: neuroprotection by selenite in the N171-82Q mouse model, Neurobiology of Disease 71 (2014) 34–42. http://dx.doi.org/10.1016/j.nbd.2014.06.022.

[24] V. Chopra, J.H. Fox, G. Lieberman, K. Dorsey, W. Matson, P. Waldmeier, D. E. Housman, A. Kazantsev, A.B. Young, S. Hersch, A small-molecule therapeutic lead for Huntington's disease: preclinical pharmacology and efficacy of C2-8 in the R6/2 transgenic mouse, Proceedings of the National Academy of Sciences

of the United States of America 104 (42) (2007) 16685–16689. http://dx.doi.org/10.1073/pnas.0707842104 17925440.
[25] J.H. Fox, D.S. Barber, B. Singh, B. Zucker, M.K. Swindell, F. Norflus, R. Buzescu, R. Chopra, R.J. Ferrante, A. Kazantsev, S.M. Hersch, Cystamine increases L-cysteine levels in Huntington's disease transgenic mouse brain and in a PC12 model of polyglutamine aggregation, Journal of Neurochemistry 91 (2) (2004) 413–422. http://dx.doi.org/10.1111/j.1471-4159.2004.02726.x 15447674.
[26] J.H. Fox, J.A. Kama, G. Lieberman, R. Chopra, K. Dorsey, V. Chopra, I. Volitakis, R. A. Cherny, A.I. Bush, S. Hersch, Mechanisms of copper ion mediated Huntington's disease progression, PLOS One 2 (3) (2007) e334. http://dx.doi.org/10.1371/journal.pone.0000334 17396163.
[27] C.J. Maynard, R. Cappai, I. Volitakis, R.A. Cherny, C.L. Masters, Q.X. Li, A.I. Bush, Gender and genetic background effects on brain metal levels in APP transgenic and normal mice: implications for Alzheimer beta-amyloid pathology, Journal of Inorganic Biochemistry 100 (5–6) (2006) 952–962. http://dx.doi.org/10.1016/j.jinorgbio.2006.02.010 16574231.
[28] D.J. Hare, A. Grubman, T.M. Ryan, A. Lothian, J.R. Liddell, R. Grimm, T. Matsuda, P.A. Doble, R.A. Cherny, A.I. Bush, A.R. White, C.L. Masters, B.R. Roberts, Profiling the iron, copper and zinc content in primary neuron and astrocyte cultures by rapid online quantitative size exclusion chromatography-inductively coupled plasma–mass spectrometry, Metallomics: Integrated Biometal Science 5 (12) (2013) 1656–1662. http://dx.doi.org/10.1039/c3mt00227f 24132241.
[29] B.R. Roberts, N.K. Lim, E.J. McAllum, P.S. Donnelly, D.J. Hare, P.A. Doble, B. J. Turner, K.A. Price, S.C. Lim, B.M. Paterson, J.L. Hickey, T.W. Rhoads, J. R. Williams, K.M. Kanninen, L.W. Hung, J.R. Liddell, A. Grubman, J.F. Monty, R. M. Llanos, D.R. Kramer, J.F. Mercer, A.I. Bush, C.L. Masters, J.A. Duce, Q.X. Li, J. S. Beckman, K.J. Barnham, A.R. White, P.J. Crouch, Oral treatment with Cu(II) (atsm) increases mutant SOD1 in vivo but protects motor neurons and improves the phenotype of a transgenic mouse model of amyotrophic lateral sclerosis, Journal of Neuroscience 34 (23) (2014) 8021–8031. http://dx.doi.org/10.1523/JNEUROSCI.4196-13.2014 24899723.
[30] E.J. Slow, J. van Raamsdonk, D. Rogers, S.H. Coleman, R.K. Graham, Y. Deng, R. Oh, N. Bissada, S.M. Hossain, Y.Z. Yang, X.J. Li, E.M. Simpson, C.A. Gutekunst, B.R. Leavitt, M.R. Hayden, Selective striatal neuronal loss in a YAC128 mouse model of Huntington disease, Human Molecular Genetics 12 (13) (2003) 1555–1567. http://dx.doi.org/10.1093/hmg/ddg169 12812983.
[31] J.H. Fox, T. Connor, V. Chopra, K. Dorsey, J.A. Kama, D. Bleckmann, C. Betschart, D. Hoyer, S. Frentzel, M. Difiglia, P. Paganetti, S.M. Hersch, The mTOR kinase inhibitor everolimus decreases S6 kinase phosphorylation but fails to reduce mutant huntingtin levels in brain and is not neuroprotective in the R6/2 mouse model of Huntington's disease, Molecular Neurodegeneration 5 (2010) 26. http://dx.doi.org/10.1186/1750-1326-5-26 20569486.
[32] J.M. Van Raamsdonk, J. Pearson, E.J. Slow, S.M. Hossain, B.R. Leavitt, M. R. Hayden, Cognitive dysfunction precedes neuropathology and motor abnormalities in the YAC128 mouse model of Huntington's disease, Journal of Neuroscience 25 (16) (2005) 4169–4180. http://dx.doi.org/10.1523/JNEUROSCI.0590-05.2005 15843620.
[33] L. Dodds, J. Chen, K. Berggren, J. Fox, Characterization of striatal neuronal loss and atrophy in the R6/2 mouse model of Huntington's disease, PLoS Currents (2014), http://dx.doi.org/10.1371/currents.hd.48727b68b39b82d5fe350f753984bcf9 24459614.
[34] E. Scherzinger, R. Lurz, M. Turmaine, L. Mangiarini, B. Hollenbach, R. Hasenbank, G.P. Bates, S.W. Davies, H. Lehrach, E.E. Wanker, Huntingtin-encoded polyglutamine expansions form amyloid-like protein aggregates in vitro and in vivo, Cell 90 (3) (1997) 549–558. http://dx.doi.org/10.1016/S0092-8674(00)80514-0 9267034.
[35] J.A. Duce, A. Tsatsanis, M.A. Cater, S.A. James, E. Robb, K. Wikhe, S.L. Leong, K. Perez, T. Johanssen, M.A. Greenough, H.H. Cho, D. Galatis, R.D. Moir, C. L. Masters, C. McLean, R.E. Tanzi, R. Cappai, K.J. Barnham, G.D. Ciccotosto, J. T. Rogers, A.I. Bush, Iron-export ferroxidase activity of beta-amyloid precursor protein is inhibited by zinc in Alzheimer's disease, Cell 142 (6) (2010) 857–867. http://dx.doi.org/10.1016/j.cell.2010.08.014 20817278.
[36] R.C. McCarthy, Y.H. Park, D.J. Kosman, sAPP modulates iron efflux from brain microvascular endothelial cells by stabilizing the ferrous iron exporter ferroportin, EMBO Reports 15 (7) (2014) 809–815. http://dx.doi.org/10.15252/embr.201338064 24867889.
[37] L. Mangiarini, K. Sathasivam, M. Seller, B. Cozens, A. Harper, C. Hetherington, M. Lawton, Y. Trottier, H. Lehrach, S.W. Davies, G.P. Bates, Exon 1 of the HD gene with an expanded CAG repeat is sufficient to cause a progressive neurological phenotype in transgenic mice, Cell 87 (3) (1996) 493–506. http://dx.doi.org/10.1016/S0092-8674(00)81369-0 8898202.
[38] E.C. Radlowski, R.W. Johnson, Perinatal iron deficiency and neurocognitive development, Frontiers in Human Neuroscience 7 (2013) 585. http://dx.doi.org/10.3389/fnhum.2013.00585 24065908.
[39] K.J. Collard, Iron homeostasis in the neonate, Pediatrics 123 (4) (2009) 1208–1216. http://dx.doi.org/10.1542/peds.2008-1047 19336381.
[40] S. Reagan-Shaw, M. Nihal, N. Ahmad, Dose translation from animal to human studies revisited, FASEB Journal 22 (3) (2008) 659–661. http://dx.doi.org/10.1096/fj.07-9574LSF 17942826.
[41] B. Clancy, B.L. Finlay, R.B. Darlington, K.J. Anand, Extrapolating brain development from experimental species to humans, Neurotoxicology 28 (5) (2007) 931–937. http://dx.doi.org/10.1016/j.neuro.2007.01.014 17368774.
[42] M. Arrasate, S. Mitra, E.S. Schweitzer, M.R. Segal, S. Finkbeiner, Inclusion body formation reduces levels of mutant huntingtin and the risk of neuronal death, Nature 431 (7010) (2004) 805–810. http://dx.doi.org/10.1038/nature02998 15483602.
[43] B. Uttara, A.V. Singh, P. Zamboni, R.T. Mahajan, Oxidative stress and neurodegenerative diseases: a review of upstream and downstream antioxidant therapeutic options, Current Neuropharmacology 7 (1) (2009) 65–74. http://dx.doi.org/10.2174/157015909787602823 19721819.
[44] M. Ribeiro, T.R. Rosenstock, T. Cunha-Oliveira, I.L. Ferreira, C.R. Oliveira, A. C. Rego, Glutathione redox cycle dysregulation in Huntington's disease knock-in striatal cells, Free Radical Biology & Medicine 53 (10) (2012) 1857–1867. http://dx.doi.org/10.1016/j.freeradbiomed.2012.09.004 22982598.
[45] B.G. Jenkins, W.J. Koroshetz, M.F. Beal, B.R. Rosen, Evidence for impairment of energy metabolism in vivo in Huntington's disease using localized 1H NMR spectroscopy, Neurology 43 (12) (1993) 2689–2695. http://dx.doi.org/10.1212/WNL.43.12.2689 8255479.
[46] A. Fredriksson, N. Schröder, P. Eriksson, I. Izquierdo, T. Archer, Neonatal iron potentiates adult MPTP-induced neurodegenerative and functional deficits, Parkinsonism & Related Disorders 7 (2) (2001) 97–105. http://dx.doi.org/10.1016/S1353-8020(00)00028-6 11248590.
[47] A.E. Millen, K.W. Dodd, A.F. Subar, Use of vitamin, mineral, nonvitamin, and nonmineral supplements in the United States: the 1987, 1992, and 2000 National Health Interview Survey results, Journal of the American Dietetic Association 104 (6) (2004) 942–950. http://dx.doi.org/10.1016/j.jada.2004.03.022 15175592.
[48] Institute of Medicine Food and Nutrition Board, Dietary Reference Intakes for Vitamin A, Vitamin K, Arsenic, Boron, Chromium, Copper, Iodine, Iron, Manganese, Molybdenum, Nickel, Silicon, Vanadium and Zinc, National Academies Press, Washington, DC, 2001.